RAPID COMMUNICATION

HDAC Activity Is Required for BDNF to Increase Quantal Neurotransmitter Release and Dendritic Spine Density in CA1 Pyramidal Neurons

Gaston Calfa,[1] Christopher A. Chapleau,[1] Susan Campbell,[1] Takafumi Inoue,[2] Sarah J. Morse,[1] Farah D. Lubin,[1] and Lucas Pozzo-Miller[1]*

ABSTRACT: Molecular mechanisms involved in the strengthening and formation of synapses include the activation and repression of specific genes or subsets of genes by epigenetic modifications that do not alter the genetic code itself. Chromatin modifications mediated by histone acetylation have been shown to be critical for synaptic plasticity at hippocampal excitatory synapses and hippocampal-dependent memory formation. Considering that brain-derived neurotrophic factor (BDNF) plays an important role in synaptic plasticity and behavioral adaptations, it is not surprising that regulation of this gene is subject to histone acetylation changes during synaptic plasticity and hippocampal-dependent memory formation. Whether the effects of BDNF on dendritic spines and quantal transmitter release require histone modifications remains less known. By using two different inhibitors of histone deacetylases (HDACs), we describe here that their activity is required for BDNF to increase dendritic spine density and excitatory quantal transmitter release onto CA1 pyramidal neurons in hippocampal slice cultures. These results suggest that histone acetylation/deacetylation is a critical step in the modulation of hippocampal synapses by BDNF. Thus, mechanisms of epigenetic modulation of synapse formation and function are novel targets to consider for the amelioration of symptoms of intellectual disabilities and neurodegenerative disorders associated with cognitive and memory deficits. © 2011 Wiley Periodicals, Inc.

KEY WORDS: epigenetics; histone deacetylase; TSA; SAHA; BDNF; quantal release; dendritic spines; hippocampal slice cultures

INTRODUCTION

Multiple learning processes allow animals to cope with environmental challenges by storing and recalling enduring modifications in the neuronal circuits that underlie adaptive behaviors (McEwen and Gianaros, 2010). The ability of the Central Nervous System (CNS) to learn is an iterative process that continually links events with outcomes until the memory of such event is formed. In this sense, for example, associative learning not only enhances the strength of existing synaptic connections between neurons, but also drives the formation of new ones (Guan et al., 2009; Restivo et al., 2009). Thus, studies of dendritic spines have gained high relevance because most excitatory synapses in the CNS are formed on these small dendritic protrusions.

Molecular mechanisms involved in the strengthening and formation of synapses include the activation and repression of specific genes or subsets of genes by stable epigenetic modifications that do not change the genetic code itself (Jiang et al., 2008). Indeed, chromatin remodeling by histone acetylation and/or DNA methylation were shown to participate in synaptic plasticity at hippocampal excitatory synapses, as well as in hippocampal-dependent learning and memory (Levenson et al., 2006; Fischer et al., 2007; Lubin et al., 2008; Guan et al., 2009). Considering the critical role that brain-derived neurotrophic factor (BDNF) plays in synaptic plasticity and behavioral adaptations (Schinder and Poo, 2000; Tyler et al., 2002; Bramham and Messaoudi, 2005) is not surprising that its gene is subject to epigenetic modifications during hippocampal-dependent learning and memory (Levenson et al., 2006; Lubin et al., 2008).

Modulation of neuronal and synaptic morphology is among the most prominent consequences of BDNF signaling. Long-term exposure to BDNF increased dendritic complexity in neurons of the cortex, cerebellum, and dentate gyrus (McAllister et al., 1995; Mertz et al., 2000; Danzer et al., 2002). In addition, BDNF increased dendritic spine density in hippocampal CA1 pyramidal neurons (Tyler and Pozzo-Miller, 2001, 2003), a process that requires intact MAPK/ERK signaling (Alonso et al., 2004). Here, we show that histone deacetylases (HDACs) activity is required for BDNF to increase dendritic spine density and excitatory quantal transmitter release onto CA1 pyramidal neurons in hippocampal slice cultures.

RESULTS

Chronic HDAC Inhibition With Trichostatin-A in Hippocampal Slice Cultures Prevents the BDNF-Induced Increase of mEPSC Frequency Recorded in CA1 Pyramidal Neurons

As we have shown previously (Tyler and Pozzo-Miller, 2001, 2003), the mean cumulative distribution of

[1] **Department of Neurobiology, Civitan International Research Center, The University of Alabama at Birmingham, Birmingham, Alabama, USA;** [2] **Department of Life Science and Medical Bioscience, Faculty of Science and Engineering, Waseda University, Tokyo 162-8480, Japan**
Grant sponsor: NIH-NINDS; Grant numbers: NS40593, NS057780, NS065027.
*Correspondence to: Lucas Pozzo-Miller, Ph.D., Department of Neurobiology, SHEL-1002, The University of Alabama at Birmingham, 1825 University Blvd., Birmingham, AL 35294-2182, USA. E-mail: lucaspm@uab.edu
Accepted for publication 13 October 2011
DOI 10.1002/hipo.20990
Published online in Wiley Online Library (wileyonlinelibrary.com).

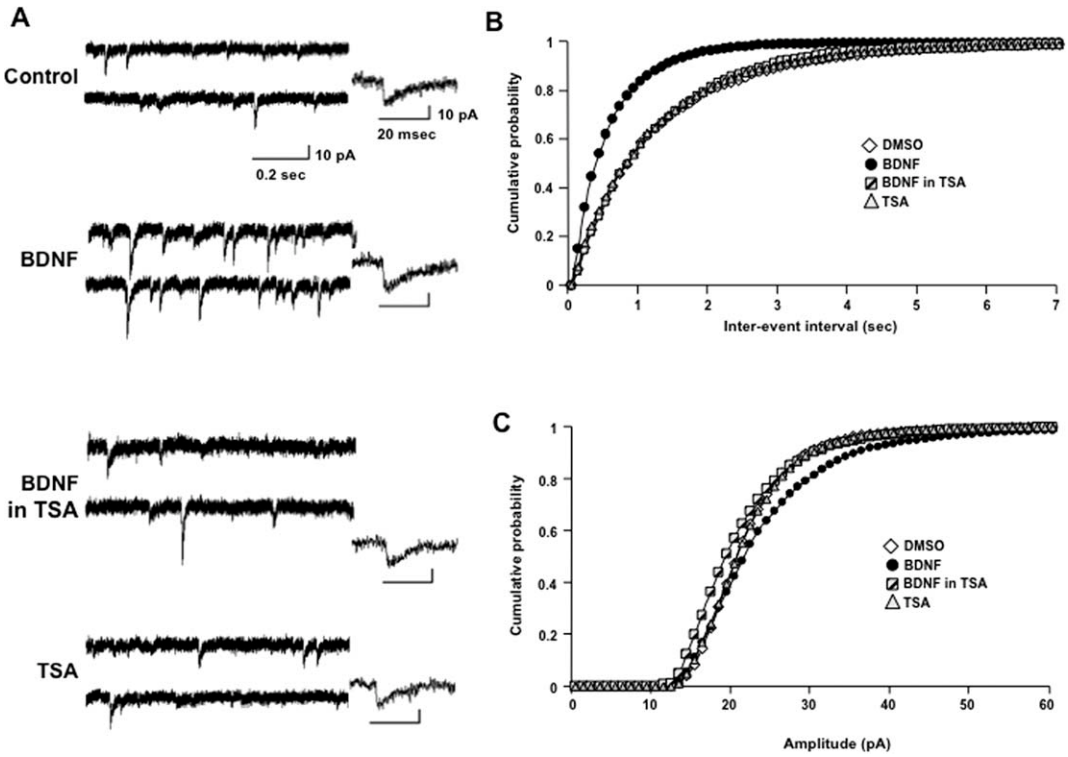

FIGURE 1. Chronic HDAC inhibition in hippocampal slice cultures prevents the BDNF-induced increase of mEPSC frequency recorded in CA1 pyramidal neurons. A: Representative continuous recording of AMPA-mediated mEPSCs from CA1 pyramidal neurons in hippocampal slice cultures exposed for 48 h to either: (1) 0.02% DMSO vehicle, (2) human recombinant mature BDNF (250 ng/mL), (3) 1.65 μM TSA dissolved in 0.02% DMSO, or (4) 250 ng/mL BDNF in the presence of 1.65 μM TSA. Insets show a representative event from each treatment group. B: Cumulative probability distributions of the inter-event intervals. C: Cumulative probability distributions of mEPSC amplitudes. $P < 0.05$ Kolmogorov–Smirnov test for comparison of cumulative probability distributions. Errors bars in cumulative probability distributions were removed for clarity.

inter-event intervals of miniature excitatory postsynaptic currents (mEPSCs) recorded in CA1 pyramidal neurons (Fig. 1A) exposed to BDNF for 48 h ($n = 5$ cells) was significantly shifted toward shorter intervals in comparison to vehicle treated controls ($n = 5$) ($P < 0.001$, Kolmogorov–Smirnov test: KS-Z value = 11.36; Fig. 1B). This shift resulted in an increase of the median (quartiles) mEPSC frequency from 0.91 Hz (0.39–0.96 Hz) in dimethyl sulfoxide (DMSO) controls to 1.57 Hz (1.25–2.82 Hz) in BDNF-treated neurons. This effect of BDNF required HDAC activity because co-exposure to trichostatin-A (TSA; 1.65 μM) resulted in a mean cumulative distribution of inter-event intervals not significantly different than that in DMSO control cells (TSA + BDNF, $n = 4$; $P = 0.3115$, KS-Z value = 0.9632), resulting in a median (quartiles) frequency of 0.78 Hz (0.69–1.13 Hz) not significantly different from DMSO controls. It should be noted that a 48 h treatment with TSA by itself had no effect on the mean cumulative distribution of inter-event intervals ($n = 3$; $P = 0.51$, KS-Z value = 0.821) and median mEPSC frequency (0.94 Hz; 0.5–1 Hz) compared to control cells. In addition, the comparison of median mEPSC frequencies between all experimental groups indicates that the distribution between groups differed significantly, which demonstrate a significant BDNF effect (Kruskal–Wallis test followed by Dunn's Multiple comparison test, KW stat = 10.19, $P = 0.017$).

Further analysis of the cumulative probability distributions of mEPSC amplitudes revealed a statistically significant rightward shift toward larger amplitude mEPSCs in BDNF-treated slices compared to all other treatments ($P < 0.05$ for each individual comparison, Kolmogorov–Smirnov test; Fig. 1C). However, differences between median (quartiles) mEPSC amplitudes were not statistically significant (DMSO 21.6 pA [21.3–23.3 pA]; BDNF 24.6 pA [17.9–28.6 pA]; TSA + BDNF 20.8 pA [18.9–22.5 pA]; TSA 21.9 pA [20.3–22.3 pA]; Kruskal–Wallis test, KW stat = 1.9, $P = 0.5923$). Since the cumulative probability distributions allow statistical comparisons across different mEPSC amplitude sizes ("bins"), these results indicate that intact HDAC activity was also necessary for BDNF to increase mEPSC amplitude.

Lastly, the kinetics of individual mEPSCs events was not affected by TSA exposure (rise times: control 2.1 ± 0.5 msec; BDNF 2.3 ± 0.4 msec; BDNF + TSA 2.2 ± 0.14 msec; TSA 2.4 ± 0.6 msec; $P > 0.05$ one-way ANOVA) (decay times: control 9.7 ± 1.2 msec; BDNF 9.9 ± 0.6 msec; BDNF + TSA 9.9 ± 0.4 msec; TSA 9.6 ± 1.2 msec; $P > 0.05$ one-way

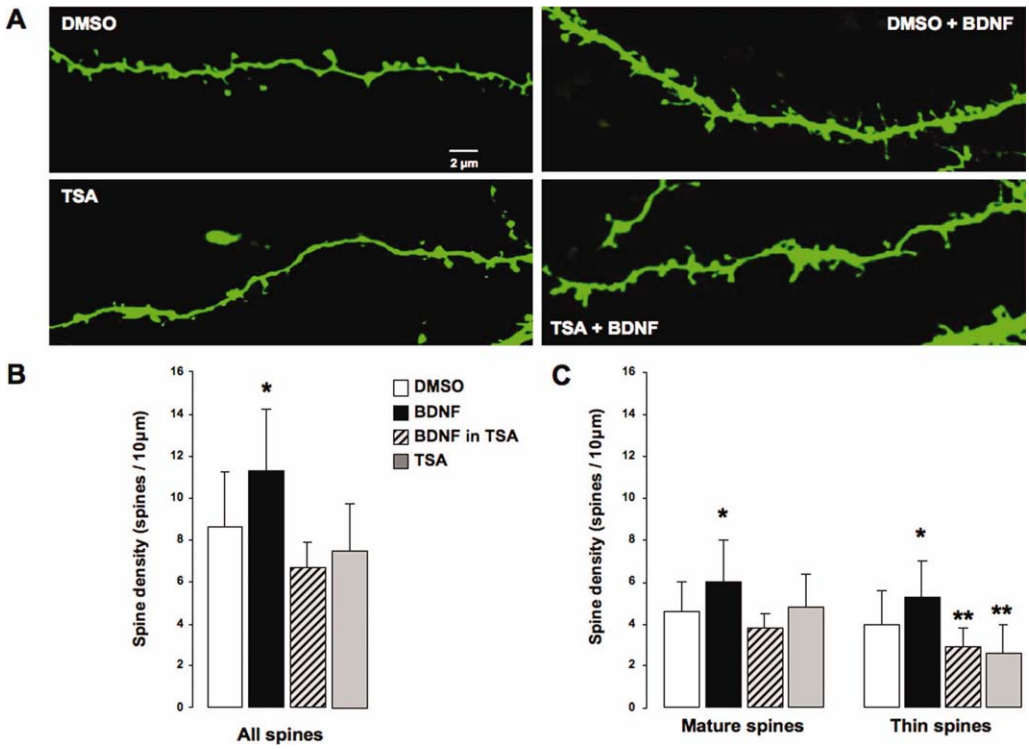

FIGURE 2. Chronic HDAC inhibition in hippocampal slice cultures prevents the BDNF-induced increase of dendritic spine density and the changes in dendritic spine morphology in CA1 pyramidal neurons. A: Representative examples of segments of secondary and tertiary branches of the apical tree of eYFP-expressing CA1 pyramidal neurons from slice cultures exposed for 48 h to either: (1) 0.02% DMSO vehicle (top left), (2) human recombinant mature BDNF (250 ng/mL; top right), (3) 1.65 µM TSA dissolved in 0.02% DMSO (bottom left), or (4) 250 ng/mL BDNF in the presence of 1.65 µM TSA (bottom right). B: Histograms of dendritic spine density, expressed as number of spines per 10 µm of apical dendrite (mean ± SD). C: Histograms of the density of each morphological type of dendritic spine per 10 µm of apical dendrite: mature-shaped spines, which included Type-I (stubby) and Type-II (mushroom) shaped spines; and immature-shaped thin spines (Type-III). *$P < 0.05$ one-way ANOVA followed by Newman–Keul test; **$P < 0.05$ one-way ANOVA followed by Newman–Keul test compared to control DMSO and BDNF-treated slice cultures. [Color figure can be viewed in the online issue, which is available at wileyonlinelibrary.com.]

ANOVA). Taken altogether, these results demonstrate that BDNF requires intact HDAC activity to enhance quantal excitatory synaptic transmission onto CA1 pyramidal neurons.

It should be noted that this concentration of the HDAC inhibitor TSA significantly increased histone H3 acetylation at K9 and K14, as determined by Western blots of TSA-treated slice cultures (285.8% of DMSO controls, $n = 4$ slice cultures in each group; $P = 0.0076$; unpaired t test with Welch's correction; Fig. 3C).

Chronic HDAC Inhibition in Hippocampal Slice Cultures Prevents the BDNF-Induced Increase of Dendritic Spine Density in CA1 Pyramidal Neurons

In addition to enhance presynaptic quantal neurotransmitter release, long-term exposure to BDNF also increased dendritic spine density in CA1 pyramidal neurons (Tyler and Pozzo-Miller, 2001, 2003; Alonso et al., 2004; Amaral and Pozzo-Miller, 2007b). To investigate the role of HDAC activity in this spinogenic effect of BDNF, hippocampal slice cultures were biolistically transfected with eYFP for 7 days *in vitro*. After 24 h of expression, slice cultures were randomly assigned to one of four experimental condition and fluorescent CA1 pyramidal neurons were imaged by laser-scanning confocal microscopy 48 h later.

Figure 2A shows representative examples of segments of secondary and tertiary branches of the apical tree of eYFP-expressing CA1 pyramidal neurons. As we showed before, BDNF (250 ng/mL) increased dendritic spine density from 8.6 ± 2.5 spines/10 µm of dendrite in DMSO controls ($n = 6$ cells) to 11.3 ± 2.9 spines/10 µm ($n = 5$; $P < 0.05$) (Fig. 2B). As with quantal excitatory synaptic transmission, this spinogenic effect of BDNF required HDAC activity, because co-incubation with 1.65 µM TSA resulted in dendritic spine density comparable to that in DMSO controls and significantly lower than in BDNF-treated slices (6.7 ± 1.2 spines/10 µm, $n = 4$; $P > 0.05$ vs. DMSO; $P < 0.05$ vs. BDNF) (Fig. 2B). It is important to note that a 48 h treatment with TSA by itself had no effect on dendritic spine density (7.5 ± 2.3 spines/10 µm, $n = 5$; $P > 0.05$ vs. DMSO) (Fig. 2B).

Using the structurally unrelated HDAC inhibitor suberoylaniline hydroxamic acid (SAHA; 1 µM) confirmed that the spinogenic effect of BDNF required intact HDAC activity

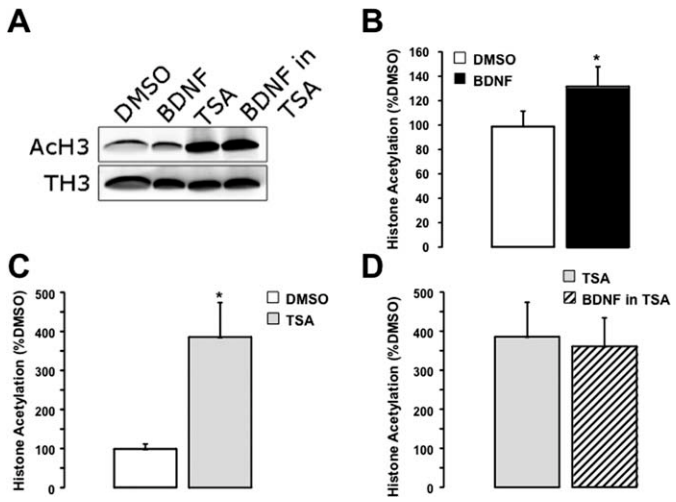

FIGURE 3. Chronic BDNF treatment of hippocampal slice cultures induced acetylation of histone H3 at lysines 9 and 14. A: Representative examples of Western immunoblots of histone 3 from whole-tissue hippocampal slices cultures treated for 48 h acetylation with DMSO (0.02%), human recombinant mature BDNF (250 ng/mL), TSA (1.65 μM), or BDNF + TSA. B: H3 acetylation at K9-K14 was increased by TSA treatment by 285.8% compared to DMSO controls. *$P = 0.0076$; unpaired t test with Welch's correction. C: BDNF increased H3 acetylation at K9-K14 by 31% compared to DMSO controls. *$P = 0.0143$; unpaired t test with Welch's correction. D: BDNF failed to induce H3 acetylation at K9-K14 when applied in the presence of TSA (−6.3% compared to TSA alone ($n = 4$; $P > 0.05$, unpaired t test with Welch's correction).

(5.4 ± 2.2 spines/10 μm, $n = 4$; $P > 0.05$ vs. DMSO). Consistent with the observations in TSA-treated slice cultures, exposure to SAHA by itself did not affect dendritic spine density (5.2 ± 1.9 spines/10 μm, $n = 7$; $P > 0.05$ vs. DMSO; $P < 0.0001$ one-way ANOVA followed by Newman–Keul test, $F(5,74) = 10.35$).

Chronic HDAC Inhibition Prevents BDNF-Induced Changes of Dendritic Spine Morphology

In addition to increase spine density, BDNF also changes the proportion of the different morphological classes of spines (Tyler and Pozzo-Miller, 2003). Here, we confirmed that BDNF-treated CA1 pyramidal neurons had 31% more "mature" spines (Type-I stubby and Type-II mushroom) than DMSO controls (5.9 ± 2 spines/10 μm vs. 4.5 ± 1.4 spines/10 μm; $P < 0.05$) (Fig. 2C). As with spine density, co-incubation with 1.65 μM TSA prevented this effect of BDNF (3.8 ± 0.7 mature spines/10 μm; $P < 0.05$) (Fig. 2C). It should be noted that exposure to TSA by itself did not affect the density of mature spines (4.8 ± 1.5 spines/10 μm, $P > 0.05$ vs. DMSO control). Consistently, SAHA also prevented the effect of BDNF on spine morphology (2.2 ± 1.1 mature spines/10 μm; $P < 0.05$). Intriguingly, SAHA by itself reduced the density of mature spines (2.3 ± 0.8 mature spines/10 μm; $P < 0.05$ vs. DMSO; $P < 0.0001$ one-way ANOVA followed by Newman–Keul test, $F(5,74) = 9.163$).

BDNF also increased the density of "immature" Type-III thin spines from 4.1 ± 1.6 spines/10 μm (DMSO control) to 5.3 ± 1.7 spines/10 μm ($P < 0.05$), an effect that was also prevented by co-application of TSA (2.9 ± 0.9 spines/10 μm; $P < 0.05$) (Fig. 2C), and SAHA (3.2 ± 1.4 spines/10 μm; $P < 0.05$). However, it should be noted that TSA reduced the density of thin spines by itself (2.6 ± 1.4 spines/10 μm; $P < 0.05$ vs. DMSO controls). On the other hand, SAHA did not change the density of "immature" spines (2.9 ± 1.2 spines/10 μm; $P < 0.05$ vs. DMSO controls) ($P < 0.0001$, one-way ANOVA followed by Newman–Keul test, $F(5,74) = 7.108$).

Taken altogether, intact HDAC activity is necessary for BDNF to modulate the density and morphology of dendritic spines in CA1 pyramidal neurons. The subtle changes in the proportion of morphological types of dendritic spines in slices exposed to HDAC inhibitors by themselves suggest that these compounds may differentially affect ongoing network activity, which in turn contribute to spine form.

Acute Inhibition of HDAC Activity Does Not Affect the Frequency, Amplitude, and Kinetics of mEPSCs Recorded in CA1 Pyramidal Neurons

To test whether TSA had any rapid (e.g., pharmacological) effects on quantal synaptic transmission, mEPSCs were also recorded from CA1 pyramidal neurons in acute slices. The cumulative probability distributions of mEPSC inter-event intervals before and after 15 min of batch application of TSA (1.65 μM) were not significantly different ($P = 0.216$, KS-Z value = 1.05; $n = 5$ cells). The median (quartiles) mEPSC frequencies were 0.2 Hz (0.16–0.39 Hz) before and 0.19 Hz (0.14–0.35Hz) after TSA (Mann–Whitney $U = 9.5$, $P = 0.55$). Similarly, the cumulative probability distribution of the mEPSCs amplitudes was not changed after 15 min of TSA application ($P = 0.6$, KS-Z value = 0.75). The median (quartiles) amplitudes were 14.4 pA (12–15.9 pA) before and 15.9 pA (12.4–27.9 pA) after TSA (Mann–Whitney $U = 8$, $P = 0.42$). Lastly, the kinetics of individual mEPSCs was not affected by TSA (rise time: control 2.32 ± 0.18 msec vs. TSA 2.28 ± 0.26 msec; $P > 0.05$; decay time: control 5.9 ± 1.1 msec vs. TSA, 5.1 ± 1.3 msec; $P > 0.05$). These observations demonstrate that the HDAC inhibitor TSA does not have pharmacological effects on quantal excitatory synaptic transmission, and the consequences of long-term exposures arise from slowly developing processes likely including epigenetic modifications.

DISCUSSION

Here, we tested whether HDAC activity was necessary for BDNF to modulate quantal excitatory synaptic transmission and dendritic spine density and morphology in CA1 pyramidal neurons. We found that co-incubation with the HDAC inhibitor

TSA prevented the effect of BDNF on mEPSC frequency and amplitude without effects of its own. In addition, TSA and SAHA abolished the effects of BDNF dendritic spine density and morphology.

As early as the later part of the 19th century and around the time when the cellular basis of brain structure was still hotly debated, Santiago Ramón y Cajal and Eugenio Tanzi speculated that the improvement of existing skills and the acquisition of new ones required structural changes in nerve cells. Currently, there is ample experimental evidence that dendritic spines, the site of most excitatory synapses in the CNS, are critically involved in the processes of learning and memory (Restivo et al., 2009). Not less important, the regulation of gene transcription has been demonstrated to participate in the establishing of new synapses and/or the strengthening of existing connections, thus contributing to long-term synaptic plasticity and memory processes (Kandel, 2001). More recently, stable epigenetic modifications that do not change the genetic code itself, such as histone acetylation and/or DNA methylation have also been shown to participate in synaptic plasticity at hippocampal excitatory synapses, as well as in hippocampal-dependent learning and memory (Levenson et al., 2006; Fischer et al., 2007; Lubin and Sweatt, 2007; Barrett and Wood, 2008; Jiang et al., 2008; Guan et al., 2009).

From the interplay between histone acetyltransferases (HAT) and HDACs enzymes, the levels of posttranslational modifications of histone tails configure the chromatin in a state that facilitate or impair the action of gene transcription machinery. HDACs remove an acetyl group from the N-terminal of the histone lysine tail, thus increasing the positive charges in the chromatin, and facilitating the binding to the phosphate backbone of DNA decreasing transcriptional activity (Turner, 2000). There are four classes of HDACs (Class I, II, III, IV), composed of 18 enzymes in the mammalian genome: Class-I includes HDAC1, 2, 3, and 8; Class-IIa is integrated by HDAC4, 5, 7, and 9; and Class-IIb includes HDAC6 and 10.

Prolonged inhibition of HDAC activity by repeated intraperitoneal injections of sodium butyrate or SAHA, which mainly inhibits Class-I and II, facilitated memory formation through a mechanism involving mainly HDAC2 (Guan et al., 2009). In addition, chronic treatment with sodium butyrate induced the reinstatement of the learning ability and recovered fear memories in a mouse model of neurodegeneration (Fischer et al., 2007). These observations suggest that chronic HDAC inhibition *in vivo* enhances synaptic transmission in brain regions involved in learning and memory. When tested in *in vitro* preparations, TSA (that is a wide spectrum HDAC inhibitor) either failed to affect excitatory synaptic transmission in acute and organotypic slices, or reduced mEPSC frequency in cultured hippocampal neurons (Akhtar et al., 2009). These apparent discrepancies could originate from the different TSA concentrations used in these studies (1 mM compared to 1.65 μM), here or the different levels of synaptic connectivity in primary cell cultures vs. organotypic slice cultures.

BDNF is the neurotrophin most studied in the context of synaptic transmission and plasticity, as well as learning and memory (Tyler et al., 2002; Bramham and Messaoudi, 2005). Indeed, endogenous BDNF is required in the parietal cortex for memory processing of a one-trial inhibitory avoidance (Alonso et al., 2005), and in CA1 of dorsal hippocampus to transform a non-lasting long-term memory trace into a persistent one trough an ERK-dependent mechanism (Bekinschtein et al., 2008). In addition, BDNF mRNA transcripts and protein are increased in the amygdala after fear conditioning and extinction (Rattiner et al., 2004a,b; Chhatwal et al., 2006; Ou and Gean, 2006). Furthermore, a different pattern of histone H3 and H4 acetylation was detected in *Bdnf* promoter 1 and 4 after fear conditioning and extinction in prefrontal cortex (Bredy et al., 2007), suggesting that enhanced *BDNF* transcription is required for the consolidation and extinction of fear conditioning. In this view, increased histone acetylation leads to enhanced *BDNF* transcription, and both promote memory consolidation. Intriguingly, the long-term actions of BDNF on synaptic transmission and spine density *in vitro* are prevented by HDAC inhibition, suggesting a complex interaction between the genes modulated by fear conditioning and those by BDNF signaling through the activation of the MAPK/CREB pathway (Segal and Greenberg, 1996). Consistent with the view that our results reflect epigenetic modifications, BDNF significantly increased H3 acetylation at K9 and K14 by 31% compared to DMSO controls in our slice cultures (BDNF $n = 5$ slices vs. DMSO $n = 4$ slices; $P = 0.0143$; unpaired t test with Welch's correction). Furthermore, BDNF-induced H3 acetylation was occluded by TSA (−6.3% compared to TSA alone; $n = 4$; $P > 0.05$, unpaired t test with Welch's correction; Fig. 3), demonstrating that the consequences of chronic HDAC inhibition on quantal synaptic transmission and dendritic spine density and morphology reflect slowly acting epigenetic modifications.

At this time, we could not exclude the possibility that the results presented here reflect the acetylation of other proteins in addition to nuclear histones. In fact, alfa-tubulin is deacetylated in Lys-40 by HDAC6 *in vitro* and *in vivo* (Hubbert et al., 2002; Zhang et al., 2003; Dompierre et al., 2007), potentially affecting dynamic microtubules within dendritic spines (Gu et al., 2008; Jaworski et al., 2009). However, it has been recently shown that WT-161, a specific inhibitor for HDAC6, did not affect memory formation to a conditional stimulus (Guan et al., 2009).

In summary, the long-term actions of BDNF hippocampal neurons, which include modulation of quantal synaptic transmission and dendritic spine density and morphology through TRPC3-mediated depolarization, intracellular Ca^{2+} signals, ERK1/2 and cAMP activation (Tyler and Pozzo-Miller, 2001, 2003; Alonso et al., 2004; Ji et al., 2005; Amaral and Pozzo-Miller, 2007a,b), also require functional HDAC activity. Our observations suggest that histone acetylation/deacetylation is a critical step in the modulation of hippocampal synapses by BDNF. Considering the current view that neurological disorders arise as a consequence of synaptic deficiencies, mechanisms of epigenetic modulation of synapse formation and function are novel targets for the amelioration of symptoms of intellectual

disabilities and neurodegenerative disorders associated with cognitive and memory deficits (Fischer et al., 2007).

DETAILED METHODS

Acute Slices

Postnatal-day 30–40 (P30–40) male rats were anesthetized with ketamine (100 mg/kg) and sacrificed by rapid decapitation. Coronal hippocampal sections (300 μm) were prepared using a vibratome (Ted Pella, Inc.) and allowed to recover for at least 1 h at room temperature in an interface holding chamber filled with artificial cerebrospinal fluid (aCSF) containing (in mM): 125 NaCl, 3.5 KCl, 1.3 $MgSO_4$, 2.5 $CaCl_2$, 26 $NaHCO_3$, and 10 D-glucose; pH 7.4; saturated with 95% O_2/5% CO_2.

Organotypic Slice Cultures

P7 rats were rapidly decapitated and the brain immersed in ice-cold Hank's balanced salt solution supplemented with glucose (41.55 mM) and antibiotic and antimycotic (1 μg/mL penicillin, 1 μg/mL streptomycin, 0.25 μg/mL amphotericin B). Both hippocampi were dissected, and 500 μm-thick transverse slices were prepared using a custom-designed tissue slicer strung with 20 μm-thick tungsten wire (California Fine Wire). After 30 min incubation at 4°C, slices were plated on tissue culture plate inserts (Millicell-CM, Millipore), fed with culture medium, and placed in an incubator at 36°C, 5% CO_2, 98% relative humidity. Culture medium consisted of 50% Minimum Essential Medium, 25% Hank's balanced salt solution, 20% heat-inactivated equine serum, 1 mM L-glutamine, and 36 mM D-glucose. After 4 days *in vitro* (DIV), the concentration of serum was titrated to serum-free over 48 h using Neurobasal-A medium (InVitrogen) supplemented with 2.5% B-27 (InVitrogen) and 1 mM L-glutamine (Tyler and Pozzo-Miller, 2003).

Transient Transfections and Treatments

After 7 DIV, cDNA plasmids encoding enhanced Yellow Fluorescent Protein (eYFP; Clontech) were introduced by biolistic gene transfer using a Helios hand-held gene-gun (Bio-Rad) (Alonso et al., 2004). After 24 h of expression, slice cultures were randomly assigned to one of six experimental conditions: (i) 0.02% DMSO (Sigma) as vehicle control; (ii) 250 ng/mL human recombinant mature BDNF (Promega); (iii) 1.65 μM trichostatin-A (TSA; Sigma) dissolved in 0.02% DMSO; (iv) 250 ng/mL BDNF in the presence of 1.65 μM TSA; (v) 1 μM SAHA (Vorinostat, Merk Co., Inc, NJ) dissolved in 0.01% DMSO; (vi) 250 ng/mL BDNF in the presence of 1 μM SAHA.

Histone Extraction and Western Blotting

Histone extractions were performed as described by Lubin and Sweatt (2007). Briefly, hippocampal slice cultures were homogenized in a Dounce Tissue Grinder (VWR) with ice-cold buffer containing (in mM): 250 sucrose, 50 Tris, pH 7.5, 25 KCl, 0.5 phenylmethylsulfonyl fluoride, 1% protease inhibitor mixture (Sigma), 0.9 Na^+-butyrate. The homogenates was centrifuged at 7,700*g* for 1 min and the pellet (nuclear fraction) was then resuspended in 0.5 mL of 0.4N H_2SO_4, incubated for 30 min and centrifuged at 14,000*g* for 10 min. The supernatant was transferred to a fresh tube, and proteins were precipitated with the addition of 250 μL of 100% trichloroacetic acid containing 4 mg/mL deoxycholic acid (Na^+ salt, Sigma) for 30 min. Acid-extracted histone proteins were then collected by centrifugation at 14,000*g* for 30 min. The protein pellet was washed with 1 mL of acidified acetone (0.1% HCl) followed by 1 mL of acetone for 5 min each. Protein precipitates were collected between washes by centrifugation (14,000*g*, 5 min). The resulting purified histone proteins were resuspended in 10 mM Tris (pH 8) and protein concentrations for each sample were determined using a DC protein assay (Bio-Rad). Aliquots of sample were then normalized to 2 μg/μL and Laemmli sample buffer (final concentration: 6.25 mM Tris, pH 6.8, 2% SDS, 10% glycerol, 1.25% 2-mercaptoethanol, 0.1% bromophenol blue) was added to histone samples before performing SDS-PAGE (12% acrylamide resolving gel overlaid with a 4% acrylamide stacking gel. Histone proteins were transferred to polyvinylidene difluoride (PVDF) membranes for immunoblotting. PVDF membranes were then incubated in the primary antibodies anti-H3-K9-K14 (1:1,000, Millipore Biotechnology) or anti-H3 (1:1,000, Abcam, US) for 1 h at room temperature. The secondary antibodies were IR-Dye goat-anti-rabbit IgG (LI-COR, Bioscience). The detection was performed in an Odyssey infrared imaging system (LI-Cor Bioscience). Ratios of Ac-H3-K9-K14 and H3 were obtained and normalized to DMSO control.

Electrophysiology

Whole-cell voltage-clamp recordings of spontaneous mEPSCs were performed in visually identified CA1 pyramidal neurons from slice cultures and acute slices. Neurons were visualized using differential interference contrast microscopy with infrared illumination (IR-DIC) using fixed-stage upright microscopes (Leica DMLFS, Zeiss Axioskop-FS). Slices were continuously perfused with aCSF containing (in mM): 122 NaCl, 2 KCl, 1.3 $MgSO_4$, 2.5 $CaCl_2$, 26 $NaHCO_3$, 10 D-glucose, and 0.5 μM TTX; pH 7.4; osmolarity was adjusted to 310 mOsm with sucrose; aCSF was continuously bubbled with 95% O_2/5% CO_2. Recordings were made at room temperature with pipettes filled with a solution containing (in mM): Cs-gluconate 120, CsCl 17.5, Na-HEPES 10, Mg-ATP 4, Na-GTP 0.4, Na_2-creatine phosphate 10, Na-EGTA 0.2 (3–5 MΩ). Typical values of access resistance after whole-cell access were <25 MΩ, and whole-cell capacitances were ~100 pF. Membrane currents were acquired and filtered (2 kHz) with an Axopatch-200B amplifier (Molecular Devices) and digitized at 4 kHz with an ITC-18 A/D-D/A interface (Instrutech) using custom-written acquisition software (TI WorkBench), or with a Digidata

1200B A/D-D/A interface using Clampex 8.0 (Molecular Devices). Digitized data were analyzed off-line with Mini-Analysis Program (Synaptosoft).

Confocal Imaging and Quantitative Analyses of Dendritic Spine Density and Morphology

Slice cultures were fixed by immersion in 4% paraformaldehyde in 100 mM phosphate buffer (PB, overnight at 4°C), and washed in PB saline (PBS). Filter membranes around each slice were trimmed, and each slice was individually mounted on glass slides and coverslipped using Vectashield (Vector Laboratories). CA1 pyramidal neurons displaying eYFP fluorescence throughout the entire dendritic tree and lacking signs of degeneration (e.g., dendritic blebbing) were selected for confocal imaging. High-resolution images of secondary and tertiary branches of apical dendrites were acquired with a Fluoview FV-300 laser-scanning confocal microscope (Olympus) using an oil immersion ×100 (NA 1.4) objective lens (PlanApo). eYFP was excited using an Ar laser (488 nm), and detected using standard FITC filters (Semrock). Series of optical sections in the *z*-axis were acquired at 0.1 μm intervals through individual apical dendritic branches. Dendritic spines were identified as small protrusions that extended ≤3 μm from the parent dendrite, and counted in maximum-intensity projections of the *z*-stacks using ImageJ (National Institutes of Health). Care was taken to ensure that each spine was counted only once by following its projection course through the stack of *z*-sections. Spines were counted only if they appeared continuous with the parent dendrite. Spine density was calculated by quantifying the number of spines per dendritic segment, and normalized to 10 μm of dendrite length.

The total length of secondary and tertiary apical dendrites analyzed was (i) DMSO controls: 714.25 μm from 19 dendritic segments of five cells; (ii) BDNF: 678.15 μm from 18 dendritic segments of six cells; (iii) BDNF + TSA: 368.45 μm from 11 dendritic segments of four cells; (iv) TSA: 565.35 μm from 16 dendritic segments of five cells; (v) SAHA: 638.6 μm from 28 dendritic segments of four cells; (vi) BDNF + SAHA: 1063.32 μm from 21 dendritic segment of eight cells.

Dendritic spines were classified either as mature-shaped spines, which included Type-I (stubby) and Type-II (mushroom) shaped spines, or immature-shaped thin spines (Type-III) based on ratios of their geometrical dimensions (length, head width, and neck width), following published criteria (Tyler and Pozzo-Miller, 2003; Boda et al., 2004; Chapleau et al., 2009).

Statistical Analyses

All data collection was performed in a blinded manner, i.e., the investigator analyzing data off-line was unaware of the treatment groups. Data are expressed as mean ± SD or median (quartiles). Group means were compared by unpaired Student's *t* test, one-way ANOVA followed by Newman–Keul test or Kruscal–Wallis test followed by Dunn's *post-hoc* test. Cumulative distribution probabilities were compared by Kolmogorov–Smirnov tests. $P < 0.05$ was considered statistically significant.

Acknowledgments

Authors thank the Alabama Neuroscience Blueprint Core Center (P30-NS57098), the UAB Intellectual and Developmental Disabilities Research Center (P30-HD38985), and the UAB Neuroscience Core (P30-NS47466) for instrumentation.

REFERENCES

Akhtar MW, Raingo J, Nelson ED, Montgomery RL, Olson EN, Kavalali ET, Monteggia LM. 2009. Histone deacetylases 1 and 2 form a developmental switch that controls excitatory synapse maturation and function. J Neurosci 29:8288–8297.

Alonso M, Medina JH, Pozzo-Miller L. 2004. ERK1/2 activation is necessary for BDNF to increase dendritic spine density in hippocampal CA1 pyramidal neurons. Learn Mem 11:172–178.

Alonso M, Bekinschtein P, Cammarota M, Vianna MR, Izquierdo I, Medina JH. 2005. Endogenous BDNF is required for long-term memory formation in the rat parietal cortex. Learn Mem 12:504–510.

Amaral MD, Pozzo-Miller L. 2007a. BDNF induces calcium elevations associated with I_{BDNF}, a nonselective cationic current mediated by TRPC channels. J Neurophysiol 98:2476–82.

Amaral MD, Pozzo-Miller L. 2007b. TRPC3 channels are necessary for brain-derived neurotrophic factor to activate a nonselective cationic current and to induce dendritic spine formation. J Neurosci 27:5179–5189.

Barrett RM, Wood MA. 2008. Beyond transcription factors: the role of chromatin modifying enzymes in regulating transcription required for memory. Learn Mem 15:460–467.

Bekinschtein P, Cammarota M, Katche C, Slipczuk L, Rossato JI, Goldin A, Izquierdo I, Medina JH. 2008. BDNF is essential to promote persistence of long-term memory storage. Proc Natl Acad Sci USA 105:2711–2716.

Boda B, Alberi S, Nikonenko I, Node-Langlois R, Jourdain P, Moosmayer M, Parisi-Jourdain L, Muller D. 2004. The mental retardation protein PAK3 contributes to synapse formation and plasticity in hippocampus. J Neurosci 24:10816–10825.

Bramham CR, Messaoudi E. 2005. BDNF function in adult synaptic plasticity: The synaptic consolidation hypothesis. Prog Neurobiol 76:99–125.

Bredy TW, Wu H, Crego C, Zellhoefer J, Sun YE, Barad M. 2007. Histone modifications around individual BDNF gene promoters in prefrontal cortex are associated with extinction of conditioned fear. Learn Mem 14:268–276.

Chapleau CA, Calfa GD, Lane MC, Albertson AJ, Larimore JL, Kudo S, Armstrong DL, Percy AK, Pozzo-Miller L. 2009. Dendritic spine pathologies in hippocampal pyramidal neurons from Rett syndrome brain and after expression of Rett-associated MECP2 mutations. Neurobiol Dis 35:219–233.

Chhatwal JP, Stanek-Rattiner L, Davis M, Ressler KJ. 2006. Amygdala BDNF signaling is required for consolidation but not encoding of extinction. Nat Neurosci 9:870–872.

Danzer SC, Crooks KR, Lo DC, McNamara JO. 2002. Increased expression of brain-derived neurotrophic factor induces formation of basal dendrites and axonal branching in dentate granule cells in hippocampal explant cultures. J Neurosci 22:9754–9763.

Dompierre JP, Godin JD, Charrin BC, Cordelieres FP, King SJ, Humbert S, Saudou F. 2007. Histone deacetylase 6 inhibition compensates for the transport deficit in Huntington's disease by increasing tubulin acetylation. J Neurosci 27:3571–3583.

Fischer A, Sananbenesi F, Wang X, Dobbin M, Tsai LH. 2007. Recovery of learning and memory is associated with chromatin remodelling. Nature 447:178–182.

Gu J, Firestein BL, Zheng JQ. 2008. Microtubules in dendritic spine development. J Neurosci 28:12120–12124.

Guan JS, Haggarty SJ, Giacometti E, Dannenberg JH, Joseph N, Gao J, Nieland TJ, Zhou Y, Wang X, Mazitschek R, Bradner JE, DePinho RA, Jaenisch R, Tsai LH. 2009. HDAC2 negatively regulates memory formation and synaptic plasticity. Nature 459:55–60.

Hubbert C, Guardiola A, Shao R, Kawaguchi Y, Ito A, Nixon A, Yoshida M, Wang XF, Yao TP. 2002. HDAC6 is a microtubule-associated deacetylase. Nature 417:455–458.

Jaworski J, Kapitein LC, Gouveia SM, Dortland BR, Wulf PS, Grigoriev I, Camera P, Spangler SA, Di Stefano P, Demmers J, Krugers H, Defilippi P, Akhmanova A, Hoogenradd CC. 2009. Dynamic microtubules regulate dendritic spine morphology and synaptic plasticity. Neuron 61:85–100.

Ji Y, Pang PT, Feng L, Lu B. 2005. Cyclic AMP controls BDNF-induced TrkB phosphorylation and dendritic spine formation in mature hippocampal neurons. Nat Neurosci 8:164–172.

Jiang Y, Langley B, Lubin FD, Renthal W, Wood MA, Yasui DH, Kumar A, Nestler EJ, Akbarian S, Beckel-Mitchener AC. 2008. Epigenetics in the nervous system. J Neurosci 28:11753–11759.

Kandel ER. 2001. The molecular biology of memory storage: a dialogue between genes and synapses. Science 294:1030–1038.

Levenson JM, Roth TL, Lubin FD, Miller CA, Huang IC, Desai P, Malone LM, Sweatt JD. 2006. Evidence that DNA (cytosine-5) methyltransferase regulates synaptic plasticity in the hippocampus. J Biol Chem 281:15763–15773.

Lubin FD, Sweatt JD. 2007. The IkappaB kinase regulates chromatin structure during reconsolidation of conditioned fear memories. Neuron 55:942–957.

Lubin FD, Roth TL, Sweatt JD. 2008. Epigenetic regulation of BDNF gene transcription in the consolidation of fear memory. J Neurosci 28:10576–10586.

McAllister AK, Lo DC, Katz LC. 1995. Neurotrophins regulate dendritic growth in developing visual cortex. Neuron 15:791–803.

McEwen BS, Gianaros PJ. 2010. Central role of the brain in stress and adaptation: links to socioeconomic status, health, and disease. Ann NY Acad Sci 1186:190–222.

Mertz K, Koscheck T, Schilling K. 2000. Brain-derived neurotrophic factor modulates dendritic morphology of cerebellar basket and stellate cells: An in vitro study. Neuroscience 97:303–310.

Ou LC, Gean PW. 2006. Regulation of amygdala-dependent learning by brain-derived neurotrophic factor is mediated by extracellular signal-regulated kinase and phosphatidylinositol-3-kinase. Neuropsychopharmacology 31:287–296.

Rattiner LM, Davis M, French CT, Ressler KJ. 2004a. Brain-derived neurotrophic factor and tyrosine kinase receptor B involvement in amygdala-dependent fear conditioning. J Neurosci 24:4796–4806.

Rattiner LM, Davis M, Ressler KJ. 2004b. Differential regulation of brain-derived neurotrophic factor transcripts during the consolidation of fear learning. Learn Mem 11:727–731.

Restivo L, Vetere G, Bontempi B, Ammassari-Teule M. 2009. The formation of recent and remote memory is associated with time-dependent formation of dendritic spines in the hippocampus and anterior cingulate cortex. J Neurosci 29:8206–8214.

Schinder AF, Poo M. 2000. The neurotrophin hypothesis for synaptic plasticity. Trends Neurosci 23:639–645.

Segal RA, Greenberg ME. 1996. Intracellular signaling pathways activated by neurotrophic factors. Annu Rev Neurosci 19:463–489.

Turner BM. 2000. Histone acetylation and an epigenetic code. Bioessays 22:836–845.

Tyler WJ, Pozzo-Miller L. 2003. Miniature synaptic transmission and BDNF modulate dendritic spine growth and form in rat CA1 neurones. J Physiol 553 (Part 2):497–509.

Tyler WJ, Pozzo-Miller LD. 2001. BDNF enhances quantal neurotransmitter release and increases the number of docked vesicles at the active zones of hippocampal excitatory synapses. J Neurosci 21:4249–4258.

Tyler WJ, Alonso M, Bramham CR, Pozzo-Miller LD. 2002. From acquisition to consolidation: on the role of brain-derived neurotrophic factor signaling in hippocampal-dependent learning. Learn Mem 9:224–237.

Zhang Y, Li N, Caron C, Matthias G, Hess D, Khochbin S, Matthias P. 2003. HDAC-6 interacts with and deacetylates tubulin and microtubules in vivo. EMBO J 22:1168–1179.